ELSEVIER Science Press

Trans. Nonferrous Met. Soc. China 19(2009) s32−s39

Transactions of Nonferrous Metals Society of China

www.tnmsc.cn

Influence of cutting parameters on surface characteristics of cut section in cutting of Inconel 718 sheet using CW Nd:YAG laser

Dong-Gyu AHN, Kyung-Won BYUN

Department of Mechanical Engineering, Chosun University, 375 Seosuk-dong, Dong-gu, Gwang-ju, 501-759, Korea

Received 2 March 2009; accepted 30 May 2009

Abstract: Recently, laser cutting technologies begin to use for manufacturing mechanical parts of Inconel super-alloy sheet due to difficulties of machining of the Inconel material as a results of its extremely tough nature. The objective of this work is to investigate the influence of cutting parameters on surface characteristics of the cut section in the cutting of Inconel 718 super-alloy sheet using CW Nd:YAG laser through laser cutting experiments. Normal cutting experiments were performed using a laser cutting system with six-axis controlled automatic robot and auto-tracking system of the focal distance. From the results of the experiments, the effects of the cutting parameters on the surface roughness, the striation formation and the microstructure of the cut section were examined. In addition, an optimal cutting condition, at which the surface roughness is minimized and both the delayed cutting phenomenon and the micro-cracking are not initiated, is estimated to improve both the part quality and the cutting efficiency.

Key words: Inconel 718 sheet; CW Nd:YAG laser; cutting parameters; surface roughness; cut and break ratio; surface qualities; optimal cutting condition

1 Introduction

The laser cutting process is a very flexible and rapid manufacturing technology with various advantages including attractive processing speed, high productivity, low running cost, ability to manufacture parts with complex shapes, excellent cut quality, non-contact operation, and ease of automation[1]. Hence, interest in the laser cutting process has greatly increased in the automobile, shipbuilding, aerospace, electronic home appliance, and nuclear industries[2]. One of the major objectives of a laser cutting process on the production line is the rapid and precise cutting of metallic sheets[3].

In order to cut metallic sheets, high-power CO_2 and Nd:YAG lasers are widely utilized. Although the CO_2 laser is commonly used in commercial sheet metal cutting processes, the merits of a Nd:YAG laser, including its lower reflectivity of the cut material, smaller kerfwidth, narrower heat affected zone, better cut edge profile, smaller thermal load, the enhanced transmission through plasma, make it an interesting application for the sheet metal cutting[4−5]. Moreover, the smaller thermal load of the Nd:YAG laser facilitates the machining of brittle materials, including nickel-based super-alloys, without crack damage in the manufactured part[5]. Inconel is nickel-based super-alloy with high strength, superior thermal resistance, distinguished wear resistance, and excellent corrosion resistance[6]. Hence, Inconel has been widely used in the manufacture of aerospace parts, gas turbine components, nuclear power plant components, shipbuilding components, and chemical equipment[7−8]. Due to the difficulty of machining Inconel material as a result of its extremely tough nature[6], laser-assisted manufacturing technologies, such as the laser welding, the laser cutting, the laser drilling, and the laser assisted machining, are commonly used to manufacture mechanical parts from Inconel [9−10].

For a laser cutting process, the productivity and the quality of the cut section are dependent on the combination of the cutting parameters, including the power of the laser, the cutting speed of the laser, the pressure of the cutting gas, and the focal position of the laser beam[11−12]. The quality of the cut section in the laser cutting of a metallic sheet can be evaluated by the

Foundation item: Project supported by a grant-in-aid of Regional Innovation Center (RIC), New Technology Development and Research Center of Laser Application in Chosun University, Korea

Corresponding author: Dong-Gyu AHN; E-mail: smart@mail.chosun.ac.kr

surface roughness, the formation of striations and the formation of the cut and break area. KARATAS et al[13] investigated the influence of the workpiece thickness and the beam waist position on the striation formation in the cutting of a hot rolled and pickled HSLA steel sheet with a thickness of 1.5 mm using a CO_2 laser. GHANY and NEWISHY[14] investigated the effects of the cutting parameters, including the pulse frequency, the duty cycle, the gas pressure, the laser power, and the cutting speed, on the surface roughness and the striation formation in the cutting of an austenitic stainless steel sheet with a thickness of 1.2 mm using pulsed and CW (Continuous wave) Nd:YAG laser. THAWARI et al[15] examined the influence of the spot overlap on the surface roughness and the surface morphology during the pulsed Nd:YAG laser cutting of a 1 mm thick Hastelloy-X sheet. Although considerable research works have been performed regarding the effects of the cutting parameters on the surface quality of the cut section during the cutting of the metallic sheets using CO_2 and Nd:YAG lasers, so far few papers associated with the laser cutting of an Inconel 718 super-alloy sheet using a CW Nd:YAG laser have been reported.

The objective of this work is to investigate the influence of cutting parameters, including the power of the laser, the cutting speed of the laser and the thickness of the workpiece, on the surface characteristics of the cut section to obtain the optimal cutting condition in the cutting of an Inconel 718 super-alloy sheet using a high-power Nd:YAG laser with continuous wave. Several cutting experiments were performed using a laser cutting system with a six-axis controlled automatic robot and an auto-tracking system of the focal distance to examine the influence of the cutting parameters on the surface roughness and the formation characteristics of the cut section. Through the observation of the cut section using an optical microscope, a scanning electron microscope (SEM) and energy dispersive X-ray (EDX), the effects of the cutting parameters on the striation formation, the cut and break areas formation and the microstructure of the cut section were investigated. Finally, the optimal cutting condition, at which the surface roughness is minimized and both the delayed cutting phenomenon and the micro-cracking are not initiated, was estimated to improve both the quality of the cut section and the cutting efficiency.

2 Experimental

Fig.1 illustrates the experimental set-up of laser cutting experiments. Laser cutting experiments were carried out using a six-axis controlled automatic robot cutting system. In order to maintain the focal distance (Z_n), as shown in Fig.1(b), at the pre-defined value during the cutting of the workpiece, an auto-tracking system (PRECITEC Inc.), which manages the focal distance, was attached to the robot laser cutting system. The focal distance was defined as the distance between the nozzle tip of the laser head and the top surface of the workpiece. In the auto-tracking system, the focal distance is controlled by the measurement of the capacitance variation between the nozzle tip and the top surface of the workpice[16]. A lamp-dumped CW Nd:YAG laser with the maximum power of 2.8 kW was utilized. The transverse mode, the wavelength and the

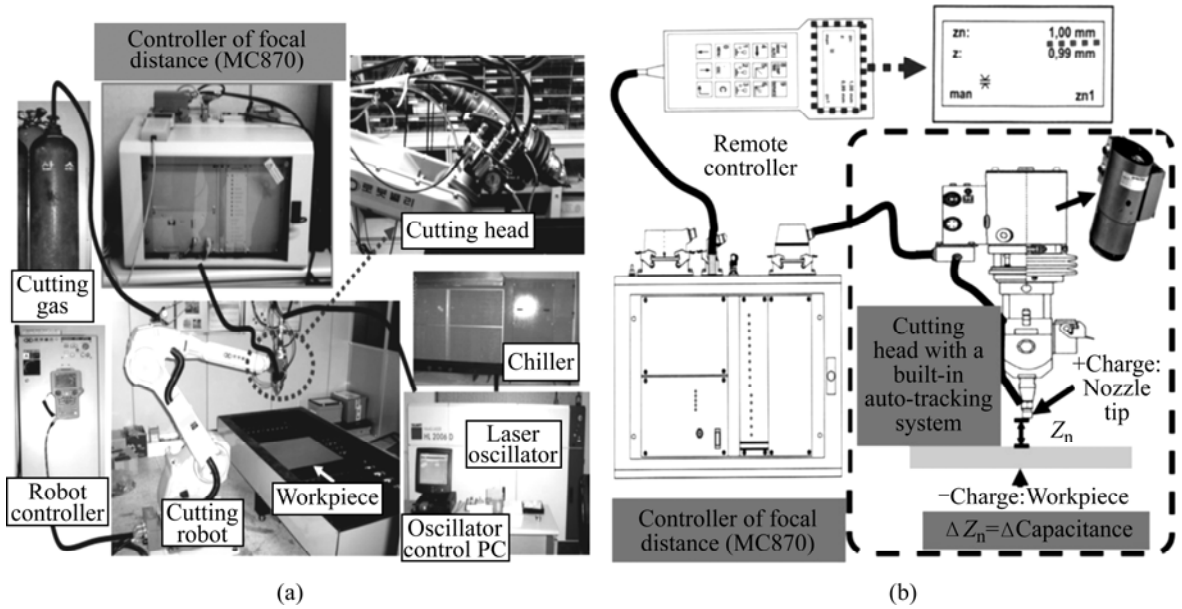

Fig.1 Experimental set-up of laser cutting experiments and schematics of auto-tracking system of focal distance: (a) Experimental set-up; (b) Schematics of auto-tracking system

spot size of the laser were TEM_{00} mode, 1.064 μm and 0.6 mm, respectively. The focal distance was set to be 1.0 mm. The focal distance with the minimum kerfwidth was chosen through preliminary tests. Oxygen gas with a purity of 99.99% was employed as an assist gas. Specimens with the length of 150 mm and the width of 30 mm were manufactured from an Inconel 718 sheet. Table 1 summarizes the chemical composition of Inconel 718.

Table 1 Chemical composition of major elements of Inconel 718 (mass fraction, %)

Ni	Cr	Fe	Mo	Nb+Ta
52.5	19.0	18.5	3.0	5.1

Several normal cutting experiments, in which the laser beam is perpendicular to the workpiece, were performed. Linear cutting of the specimen was carried out in the longitudinal direction. The power of the laser (P), the cutting speed of the laser (v) and the thickness of the workpiece (d) were selected as the cutting parameters. The experimental conditions are shown in Table 2. The pressure of the assist gas was 0.1 MPa.

The surface roughness of the cut section was measured by a roughness tester equipped with a stylus instrument (Surftest 402). The morphology, the striation formation and the cut and break characteristics of the cut section were observed via the optical microscope, SEM and EDX. The measured surface roughness was the average absolute value of the profile deviation from the mean line (R_a) and the maximum roughness (R_{max}). The surface roughness was measured in the center of the cut specimen in the thickness direction.

Table 2 Experimental conditions

Thickness of workpiece/mm	Power of laser/kW	Cutting speed of laser/(m·min^{-1})	Pressure of assist gas/MPa
1.0	1.4−1.8	5−10	0.1
1.6	1.4−1.6	3−7	0.1
1.6	1.8	3−8	0.1
2.0	1.4 −1.8	3−6	0.1

3 Results and discussion

3.1 Surface roughness

Fig.2 shows the influence of the cutting speed of the laser, the power of the laser and the thickness of the workpiece on the average absolute value of the profile deviation from the mean line and the maximum roughness of the cut section. Table 3 shows the minimum and maximum values of the surface roughness for each combination of the laser power and the workpiece thickness.

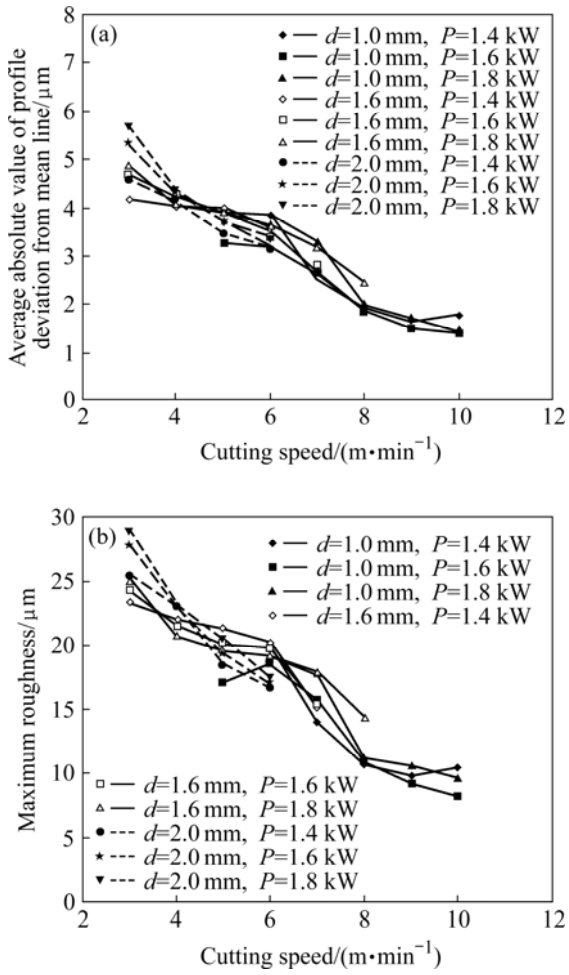

Fig.2 Influence of cutting speed and power of laser on average absolute value of profile deviation from mean line and maximum roughness for different workpiece thicknesses: (a) Average absolute value of profile deviation from mean line; (b) Maximum roughness

Fig.2 and Table 3 show that the values of the average absolute value of the profile deviation from the mean line and the maximum roughness lie within the ranges of 1.4−5.7 μm and 8.2−29.1 μm, respectively. This result is nearly three times larger than the result of the cutting of mild steel with an identical thickness using a CW Nd:YAG laser[17]. This is because the composition of the Inconel 718 includes more reactive ingredients, such as chromium, nickel and niobium, than the mild steel and the heat energy caused by the oxidation reaction between the oxygen gas and the increased reactive ingredients produces deeper grooves with larger peaks and valleys in the cut section of Inconel 718.

Fig.2 shows that the variation of the surface roughness of cut section according to the laser power is less than 0.7 μm of the average absolute value of the profile deviation from the mean line and 3.0 μm of the

Table 3 Ranges of surface roughness for different workpiece thicknesses

Thickness/mm	Power of laser/kW	Average absolute value of profile deviation from mean line/μm		Maximum roughness/μm	
		Minimum	Maximum	Minimum	Maximum
1.0	1.4	1.8	3.9	10.4	20.0
	1.6	1.4	3.3	8.2	18.6
	1.8	1.5	3.9	9.8	19.8
1.6	1.4	2.7	4.2	15.1	23.5
	1.6	2.8	4.7	15.4	24.4
	1.8	2.5	4.9	14.5	25.2
2.0	1.4	3.1	4.6	16.7	25.5
	1.6	3.2	5.4	17.1	27.7
	1.8	3.5	5.7	17.6	29.1

maximum roughness. Fig.2 shows that the influence of the workpiece thickness on the surface roughness is less than 0.7 μm of the average absolute value of the profile deviation from the mean line and 3.5 μm of the maximum roughness at an identical cutting speed. From these results, it is noted that the laser power and the workpiece thickness scarcely affect the variation of the surface roughness of the cut section. Fig.2 shows that the surface roughness decreases nearly in inverse proportion to the cutting speed of the laser. In addition, the region of the cutting speed with nearly identical surface roughness is generated after a region associated with a rapid decrease of the surface roughness as the cutting speed increases. From Fig.2, it can be seen that the surface roughness increases remarkably at a laser cutting speed of 3 m/min and at a laser power greater than 1.6 kW. This may be ascribed to the fact that the sideways burning phenomenon, in which the side burning of the cut section caused by an oxidation reaction between the oxygen gas and the cut material increases the melting depth in the normal direction of the cut section when the cutting speed of the laser is less than the speed of the oxidation reaction front[18], occurs as the cutting speed is less than 3 m/min.

3.2 Formation of striation and cut and break areas

Fig.3 shows the influence of the power and the cutting speed of the laser on the formation of striations on the cut section. From Fig.3, it is observed that the striation of the cut section changes from a long period profile with a large height to a short period profile with a small height as the cutting speed increases. This may be ascribed to the decrease of the surface roughness with increasing the cutting speed. Moreover, Fig.3 shows that the striation of the cut section forms nearly similar patterns irrespective of the laser power.

Fig.4 shows the effects of the cutting parameters on the formation of the cut and break areas on the cut section. From Fig.4, it can be seen that the break area, which is formed on the lower surface of the cut section due to the insufficient supply of the heat input, increases as the cutting speed of the laser increases and the power of the laser decreases. In addition, it is observed that the delayed cutting phenomenon with pronounced slopes of the striations due to the insufficient heat input occurs in the break area of the cut section at high cutting speed regions. Through the investigation of a cross-section of the cut specimen, it is found that a vertical cross-section is created in the lower region of the cut section when the delayed cutting phenomenon initiates.

Inverse effective heat input (ξ) is introduced as Eq.(1) to consider the effects of the cutting speed and the laser power on the height of the break area, together. In order to formulate an empirical equation for the relationship between the inverse effective heat input and the height of the break area, data fittings were carried out using the linear regression method in the following form:

$$\chi = \lambda_1 \xi + \lambda_2 = \lambda_1 \frac{v}{\sqrt{P}} + \lambda_2 \quad (1)$$

where χ, ξ, v, P and λ_i denote the height of the break area, the inverse effective heat input, the cutting speed of the laser, the power of the laser, and the coefficients of the linear equations, respectively.

Fig.5 represents the relationship between the inverse effective heat input and the height of the break area. Table 4 shows the coefficients of the linear regression equation and its correlation coefficient (R^2). Fig.5 shows that the height of the break area increases linearly in proportion to the inverse effective heat input. From Table 4, it can be seen that the correlation coefficient at each thickness of the workpiece is greater

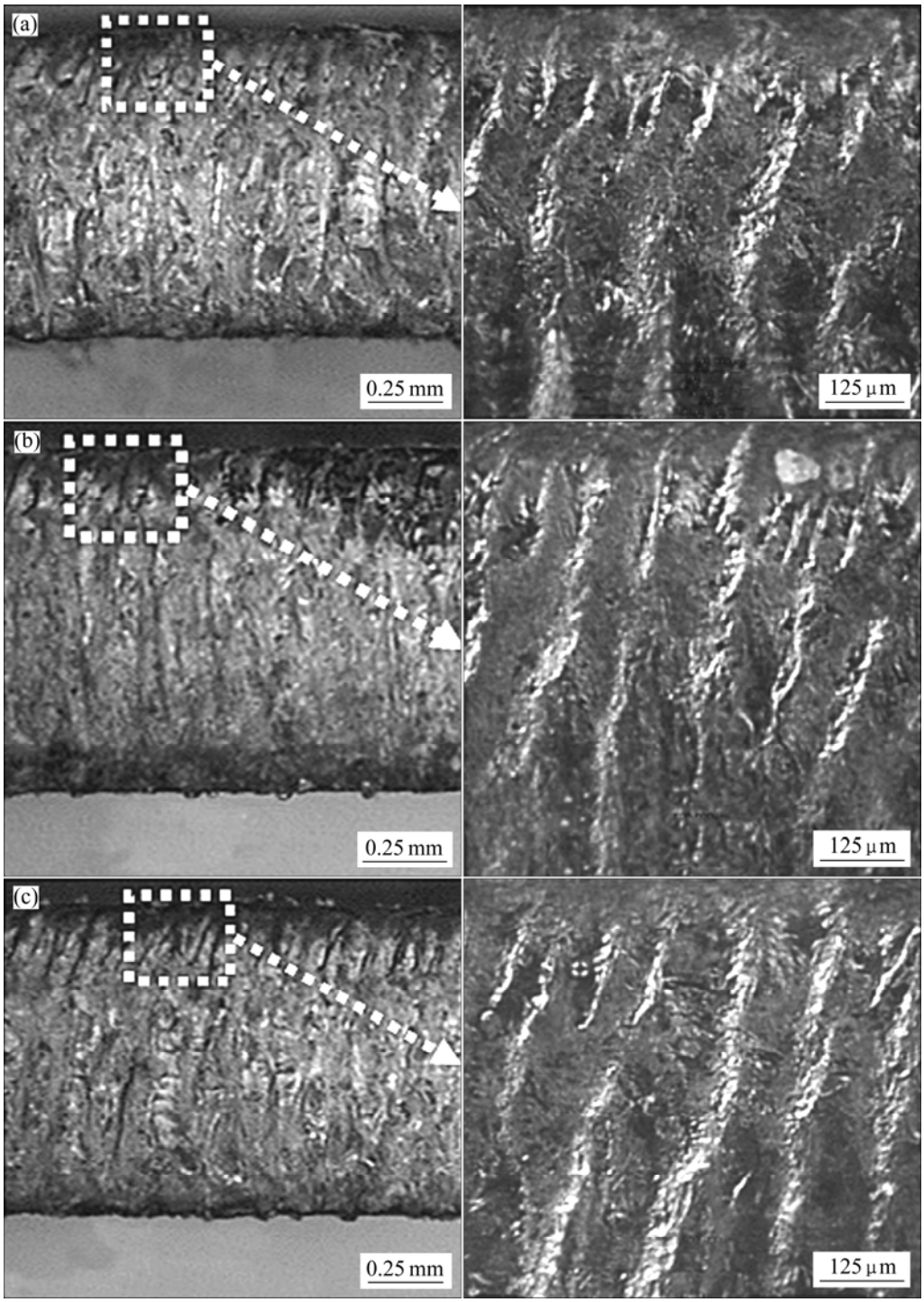

Fig.3 Effects of cutting parameters on striation formation on cut section (d=1.0 mm): (a) P=1.4 kW, v=5 m/min; (b) P=1.4 kW, v=7 m/min; (c) P=1.8 kW, v=5 m/min

Table 4 Coefficients of relationship between inverse effective heat input and height of break area for different workpiece thicknesses

Thickness/mm	λ_1/(J$^{0.5}$·s$^{0.5}$)	λ_2/mm	Correlation coefficient
1.0	0.003 1	−0.181	0.92
1.6	0.004 1	0.281	0.96
2.0	0.006 5	0.594	0.94

than 0.9. This implies that the relationship between the inverse effective heat input and the height of the break area has a strong linearity.

3.3 Microstructures

Fig.6 shows microstructures and morphologies in the vicinity of the cut and break areas. Fig.6(a) shows that the oxides are formed on the cut area due to an

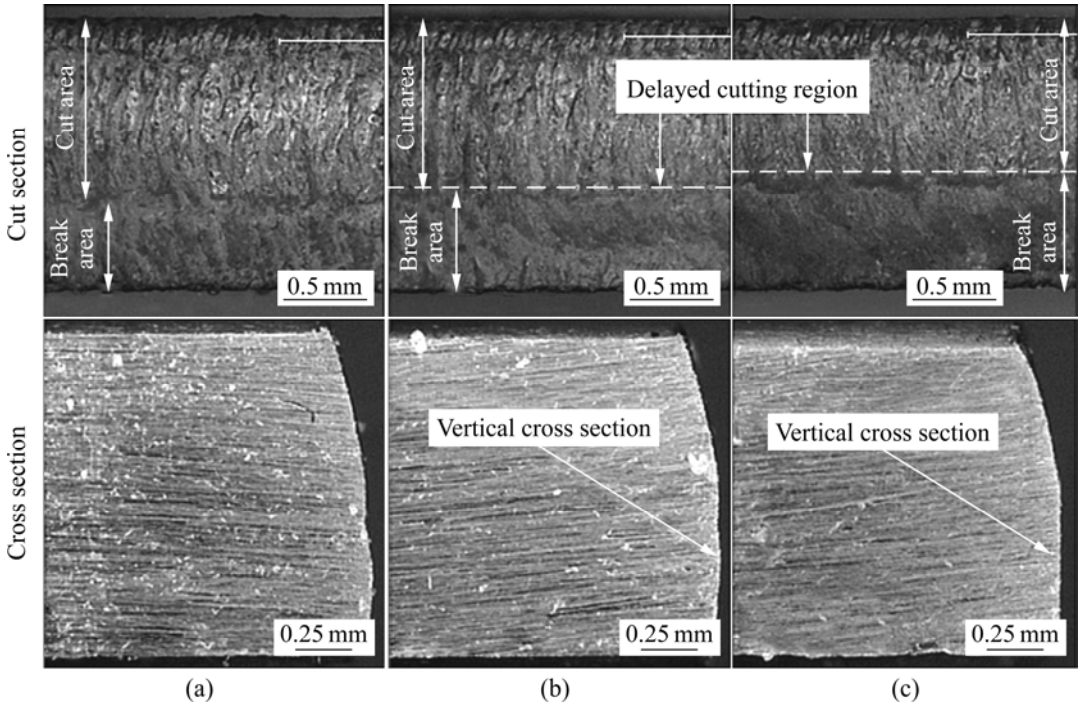

Fig.4 Effects of cutting parameters on formation of cut and break areas on cut section (d=1.6 mm and P=1.8 kW): (a) v=6 m/min; (b) v=7 m/min; (c) v=8 m/min

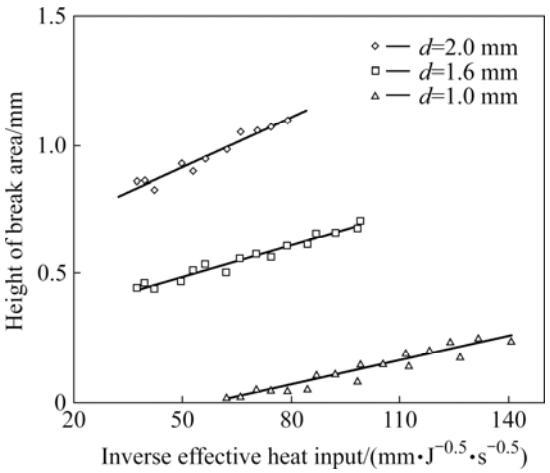

Fig.5 Relationship between inverse effective heat input and height of break area

oxidation reaction between the oxygen gas and the molten metal in the kerfwidth. In addition, it is observed that micro-cracks are created in the valleys of the striations when the delayed cutting phenomenon occurs. From the investigation of the microstructures and morphologies in the vicinity of the break area, it is observed that the break area is covered with the oxides, which pour down from the cut area, as shown in Fig.6(b).

The compositions of the oxides in the cut and break areas were analyzed via the EDX. The results of the composition analysis of the oxides showed that Cr_2O_3 and Nb_2O_5 are the major compounds of the oxides, as shown in Fig.6. In addition, it is observed that the composition of Cr_2O_3 increases from 60.5% to 71.4% as the measured region of the cut section shifts from the cut area to the break area.

3.4 Optimal cutting condition

Through the investigation of the results of the experiments, the optimal cutting condition for each thickness of the workpiece was estimated. The quality of laser cutting parts is highly dependent on the surface roughness of the cut section. According to the results of the experiments, it shows that the surface roughness decreases when the cutting speed increases. However, in order to obtain the high quality parts using the laser cutting process, the delayed cutting phenomenon, excessive dross attachment and micro-cracks should not be created in the cut section. Hence, the optimal cutting conditions were determined as the maximum cutting speeds, at which the delayed cutting phenomenon and the formation of micro-cracks on the cut section are not observed, for each combination of the laser power and the workpiece thickness, as shown in Table 5.

Table 5 shows that the surface roughness of the cut section lies in the ranges of 1.8−4.2 μm of the average absolute value of the profile deviation from the mean line and 11.1−23.2 μm of the maximum roughness at each optimal cutting condition.

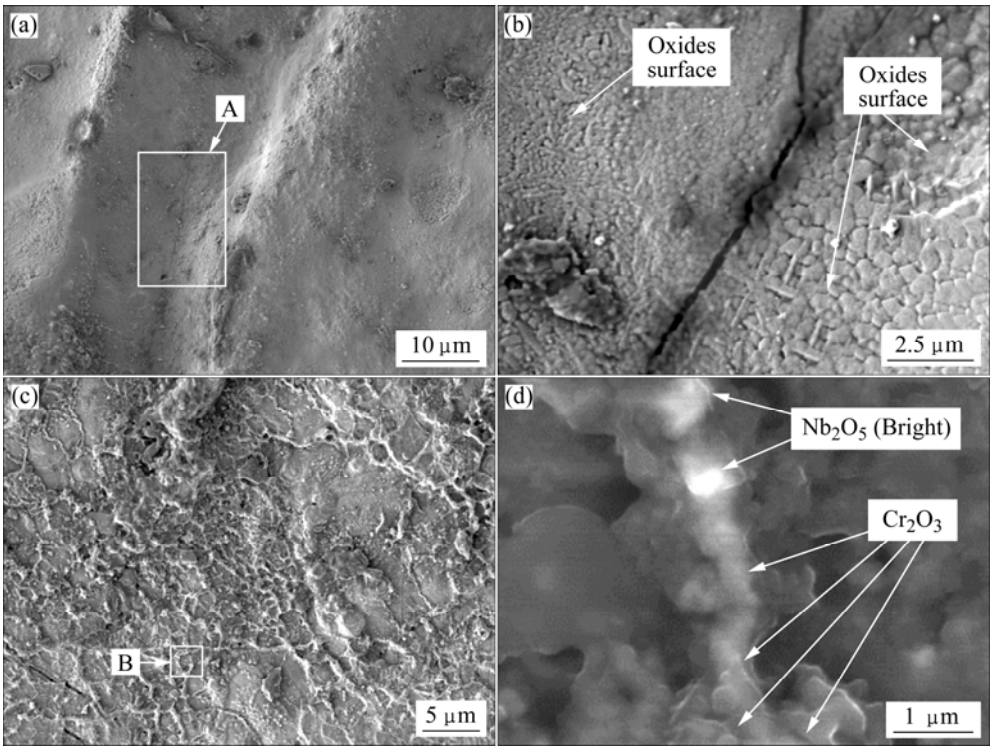

Fig.6 Microstructures and morphologies in vicinity of cut and break areas (d=1.6 mm, P=1.6 kW and v=7 m/min): (a) Morphology of cut area; (b) Microstructures of region A; (c) Morphology of break area; (d) Microstructures of region B

Table 5 Surface roughness and height of break area for each optimal cutting condition

Thickness/mm	Power of laser/kW	Optimal cutting speed/(m·min^{-1})	Average absolute value of profile deviation from mean line/μm	Maximum roughness/μm	Height of break area/mm
1.0	1.4	7	2.4	14.1	0.14
	1.6	8	1.8	11.1	0.20
	1.8	8	2.0	11.3	0.19
1.6	1.4	5	4.0	21.4	0.57
	1.6	6	3.4	19.9	0.61
	1.8	6	3.7	19.1	0.56
2.0	1.4	4	4.2	23.2	0.95
	1.6	5	3.7	19.4	1.05
	1.8	5	3.6	20.7	0.98

4 Conclusions

1) The experimental results of the cutting of Inconel 718 using a CW Nd:YAG laser show that the variation of the surface roughness of the cut section is affected mainly by the cutting speed. In addition, the values of the average absolute value of the profile deviation from the mean line and the maximum roughness lie in the ranges of 1.4−5.7 μm and 8.2−29.1 μm, respectively.

2) The observation results of the variation of the formation of the striations and the cut and break area on the cut section according to the cutting parameters show that the striation of the cut section changes from a long period profile to a short period profile as the cutting speed increases. Moreover, it is observed that the delayed cutting phenomenon with pronounced striation slopes occurs in the break area at high cutting speed regions.

3) The relationship between the inverse effective heat input and the height of the break area is estimated using a linear regression method.

4) The investigation of the microstructures and the composition of the oxides on the cut and break areas shows that similar oxides, which mainly consist of Cr_2O_3 and Nb_2O_5, are formed on both the cut area and the break areas. Moreover, the micro-cracks are created in valleys

of the striations as the delayed cutting phenomenon occurs. In addition, it is found that the oxides on the cut area are created from an oxidation reaction between the oxygen gas and the molten metal in the kerfwdith; but on the other hand, the oxide blankets cover the break area due to the pouring down of the molten oxides in the cut area.

5) Based on these results, the optimal cutting condition, at which the surface roughness is minimized and both the delayed cutting phenomenon and the micro-cracking are not initiated, is estimated to improve both the quality of the cut section and the cutting efficiency.

References

[1] WOLLERMANN-WINDGASSE R, SCHINZEL C. Laser technology in manufacturing-state of the art at the beginning of the 21st century [C]// LANE 2001. Erlangen, 2001: 87−102.

[2] GEIGER M. Manufacturing science-driving force for innovation [C]// The 7th International Conference on Technology of Plasticity. Yokohama, 2002: 17−30.

[3] HAN G C, NA S J. A study on torch path planning in laser cutting process Part 2: Cutting path optimization using simulated annealing [J]. Journal of Manufacturing Processes, 1999, 18(2): 62−70.

[4] AHN D G, PARK H J. Investigation into thermal characteristics in cutting of a low carbon sheet using a high-power CW Nd:YAG laser for net shape manufacturing [J]. Key Engineering Materials, 2007, 344: 169−176.

[5] DUBEY A K, YADAVA V. Experimental study of Nd:YAG laser beam machining—An overview [J]. Journal of Materials Processing Technology, 2008, 195: 15−26.

[6] RAHMAN M, SEAH W K H, TEO T T. The machinability of Inconel 718 [J]. Journal of Material Processing Technology, 1997, 63: 199−204.

[7] PAWADE R S, JOSHI S S, BRAHMANKAR P K. Effect of machining parameters and cutting edge geometry on surface integrity of high-speed turned Inconel 718 [J]. International Journal of Machine Tools & Manufacture, 2008, 48: 15−28.

[8] HAN W J, BYEON J G, PARK K S. Welding characteristics of the Inconel plate using a pulsed Nd:YAG laser beam [J]. Journal of Material Processing Technology, 2001, 113: 234−237.

[9] ANDERSON M, PATWA R, SHIN Y C. Laser-assisted machining of Inconel 718 with an economic analysis [J]. International Journal of Machine Tools & Manufacture, 2006, 46: 1879−1891.

[10] CHIEN W T, HOU S C. Investigating the recast layer formed during the laser trepan drilling of Inconel 718 using the Taguchi method [J]. International Journal of Advanced Manufacturing Technology, 2007, 33: 308−316.

[11] GHANY K A, RAFEA H A, NEWISHY M. Using a Nd:YAG laser and six axes robot to cut zinc-coated steel [J]. International Journal of Advanced Manufacturing Technology, 2006, 28: 1111−1117.

[12] SOBIH M, CROUSE P L, LI L. Striation-free fiber laser cutting of mild steel sheets [J]. Applied Physics A—Materials Science & Processing, 2008, 90: 171−174.

[13] KARATAS C, KELES O, USLAN I, USTA Y. Laser cutting of steel sheets: Influence of workpiece thickness and beam waist position on kerf size and stria formation [J]. Journal of Material Processing Technology, 2006, 172: 22−29.

[14] GHANY K A, NEWISHY M. Cutting of 1.2 mm thick austenitic stainless steel sheet using pulsed and CW Nd:YAG laser [J]. Journal of Material Processing Technology, 2005, 168: 438−447.

[15] THAWARI G, SARIN SUNDAR J K, SUNDARARAJAN G, JOSHI S V. Influence of process parameters during pulsed Nd:YAG laser cutting of nickel-base superalloys [J]. Journal of Material Processing Technology, 2005, 170: 229−239.

[16] BIERMANN S, TOPKAYA A, JAGIELLA M. Capacitance clearance sensor system for high quality Nd:YAG laser cutting and welding of sheet metals [C]// European Conference on Laser Treatment of Materials. Göttingen, 1992: 51−56.

[17] AHN D G, KIM M S, YOO Y T, PARK H J. Effects of process parameters on surface characteristics in cutting of cold rolled steel sheets using a high-power CW Nd:YAG laser [J]. Materials Science Forum, 2008, 580/582: 455−458.

[18] PIETRO P D, YAO Y L. An investigation into characterizing and optimizing laser cutting quality—A review [J]. International Journal of Machine Tools & Manufacture, 1994, 34: 225−243.

(Edited by YANG You-ping)